energies

Review

Recent Advances in the Use of Sodium Borohydride as a Solid State Hydrogen Store

Jianfeng Mao and Duncan H. Gregory *

WestCHEM, School of Chemistry, University of Glasgow, Joseph Black Building, Glasgow G12 8QQ, UK; E-Mail: jfmao@umd.edu

* Author to whom correspondence should be addressed; E-Mail: duncan.gregory@glasgow.ac.uk; Tel.: +44-141-330-6438; Fax: +44-141-330-4888.

Abstract: The development of new practical hydrogen storage materials with high volumetric and gravimetric hydrogen densities is necessary to implement fuel cell technology for both mobile and stationary applications. $NaBH_4$, owing to its low cost and high hydrogen density (10.6 wt%), has received extensive attention as a promising hydrogen storage medium. However, its practical use is hampered by its high thermodynamic stability and slow hydrogen exchange kinetics. Recent developments have been made in promoting H_2 release and tuning the thermodynamics of the thermal decomposition of solid $NaBH_4$. These conceptual advances offer a positive outlook for using $NaBH_4$-based materials as viable hydrogen storage carriers for mobile applications. This review summarizes contemporary progress in this field with a focus on the fundamental dehydrogenation and rehydrogenation pathways and properties and on material design strategies towards improved kinetics and thermodynamics such as catalytic doping, nano-engineering, additive destabilization and chemical modification.

Keywords: hydrogen; hydride; sodium borohydride; hydrogen storage

1. Introduction

With concerning current trends in environmental pollution and depletion of fossil energy resources, there is an imperative to seek renewable and clean energy sources that can support the continued

sustainable development of human society. Hydrogen is regarded as one of the best alternative sustainable energy carriers because of its abundance, high energy density and lack of adverse environmental impact (for example, when oxidized as water). However, an important challenge for the use of hydrogen for mobile (e.g., automotive) and small scale energy generation is how to achieve safe, cheap, high density storage [1]. Essentially, hydrogen can be stored either in a physical form (as a gas or liquid) or in a chemical form (e.g., within metal hydrides or so-called chemical hydrides). Compressed gas and liquid hydrogen storage technologies represent the current state-of-the art, but more compact (gravimetrically and/or volumetrically efficient) means of storing hydrogen are needed for mobile applications on a practical level. In principle, solid state hydrogen storage in metal hydrides is considered a more effective and safer way to handle hydrogen than its storage as either a compressed gas or cryogenic liquid. The hydrides offer volumetric hydrogen densities substantially greater than that of compressed gas and comparable to or exceeding that of liquid hydrogen but without the requirement of very high pressure containment vessels or cryogenic tanks [2–4]. An ideal on-board hydrogen storage material will have a low molar weight, be inexpensive, have rapid kinetics for absorbing and desorbing H_2 in the 25–120 °C temperature range, and store large quantities of hydrogen reversibly [5]. Recently, light metal borohydrides such as $NaBH_4$ [6–8], $LiBH_4$ [9–12], $Mg(BH_4)_2$ [13–15], and $Ca(BH_4)_2$ [16–18] have attracted much attention as potential hydrogen storage media primarily due to their high gravimetric capacities. The physical and chemical properties of these borohydrides are shown in Table 1 [19,20]. Perhaps compared to the borohydrides of lithium, magnesium and calcium there has been little focus on $NaBH_4$ for hydrogen storage in the solid state due to its relatively much higher decomposition temperature. Given that the decomposition temperature of $NaBH_4$ at 1 bar of H_2 is in excess of 500 °C, the required operating temperature for a store would considerably exceed that required for practical application in hydrogen fuel cell vehicles [7]. This fact alone explains why most previous research has been conducted on the hydrolysis of $NaBH_4$ for hydrogen generation rather than its thermolysis as part of a solid state storage system [21]. However, the gravimetric hydrogen storage capacity of real hydrolysis-based storage systems will invariably be lower than the theoretical 10.6 wt% figure due to the excess water required to dissolve the $NaBH_4$ and its by-product, $NaBO_2$, as well as the added mass of the reaction and storage vessels. Hence, the U.S. Department of Energy (US DOE) issued a "No-Go" recommendation for the hydrolysis of $NaBH_4$ in 2007, and since then the approach has no longer been seriously considered for automotive applications [22].

Table 1. Physical and chemical properties of borohydrides.

Borohydride	Cost [a]/(USD/g)	Hydrogen density/wt%	T_d [b]/ °C	Reaction	References
$NaBH_4$	6.47	10.6	505	$NaBH_4 \rightarrow Na + B + 2H_2$	[6–8]
$LiBH_4$	15.65	18.5	380	$LiBH_4 \rightarrow Li + B + 2H_2$	[9–12]
$Mg(BH_4)_2$	116.5	14.9	320	$Mg(BH_4)_2 \rightarrow MgB_2 + 4H_2$	[13–15]
$Ca(BH_4)_2$	142	11.6	367	$Ca(BH_4)_2 \rightarrow 2/3CaH_2 + 1/3CaB_6 + 10/3H_2$	[16–18]

[a] Prices from Sigma-Aldrich [23] for hydrogen storage grade materials; and [b] dehydrogenation temperature.

However, use of solid NaBH$_4$ for hydrogen storage has many advantages. Compared to other borohydrides, NaBH$_4$ is cheaper and relatively stable in air [24]. For NaBH$_4$ to be suitable for practical applications, the desorption temperature must be reduced and appreciable cyclability must be demonstrated. Over the last several years some novel strategies such as catalysis, nano-engineering, additive destabilization and chemical modification have been employed to address the thermodynamic and kinetic limitations of the thermal decomposition of NaBH$_4$. While NaBH$_4$ is not yet the solution to the problem of facile storage of hydrogen in the solid state, the progress of the various methodologies in improving both performance and understanding of this performance has been highly encouraging and hence we focus on these advances in this review. The primary purpose of this paper is to consider progress largely from 2009 onwards, comparing what is known regarding the decomposition behavior and mechanism of pristine NaBH$_4$ with materials modified using the approaches listed above and the prospects of such systems for practical exploitation.

2. Thermal Decomposition

NaBH$_4$ adopts a NaCl-type structure at ambient conditions in which four hydrogen atoms are covalently stabilized within the BH$_4^-$ anion, which in turn is bonded essentially ionically to the counter-cation Na$^+$ [24]. The complete hydrogen desorption reaction of NaBH$_4$ can be expressed as follows:

$$NaBH_4 \rightarrow Na + B + 2H_2 \qquad 10.6\ wt\% \qquad (1)$$
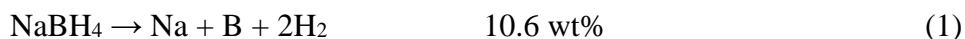
However, like many other borohydrides, the real decomposition process of NaBH$_4$ is likely to be more complex and involve intermediate phases such as NaH, Na$_2$B$_{12}$H$_{12}$, or even release impurity gases such as B$_2$H$_6$ [6]. Recent theoretical and experimental studies have provided insight into its decomposition behavior as well as identifying the extent of the challenges ahead in developing NaBH$_4$ as a viable hydrogen carrier.

First principles calculations suggest a scenario where BH$_4^-$ ions decompose at the surface of NaBH$_4$ into H$^-$ ions and BH$_3$ molecules [25]. The H$^-$ ions remain in the lattice, locally converting NaBH$_4$ into NaH. The BH$_3$ molecules originating from the decomposition can escape to the gas phase and form B$_2$H$_6$ (diborane) molecules, for instance. Alternatively, they may decompose immediately to form hydrogen and B. However, there is no direct evidence from mass spectrometry data of B$_2$H$_6$ release during the decomposition of NaBH$_4$ [6]. Despite this lack of experimental evidence, it remains possible that NaBH$_4$ decomposition may involve diborane emission, as is seen in the thermal decomposition of less stable borohydrides [20]. Due to the high temperature necessary for decomposition on the one hand and the low thermal stability of diborane on the other, most of the diborane decomposes into the elements. At the same time, some of the gaseous species may react with remaining NaBH$_4$ to form Na$_2$B$_{12}$H$_{12}$.

Martelli *et al.* [7] investigated the stability and hydrogen desorption of NaBH$_4$ via dynamic pressure, composition, and temperature (PCT) measurements under constant hydrogen flows. It was found that only one plateau is visible in the isotherms, indicating that the decomposition occurs in one step (Figure 1). From the van't Hoff equation, the enthalpy and entropy of reaction are -108 ± 3 kJ mol^{-1} of H$_2$ and 133 ± 3 J K^{-1} mol^{-1} of H$_2$ respectively. This corresponds to a decomposition temperature,

$T_d = 534 \pm 10$ °C at 1 bar of H_2. The high stability of $NaBH_4$ leads to a dehydrogenation temperature that is above the decomposition temperature of NaH [26].
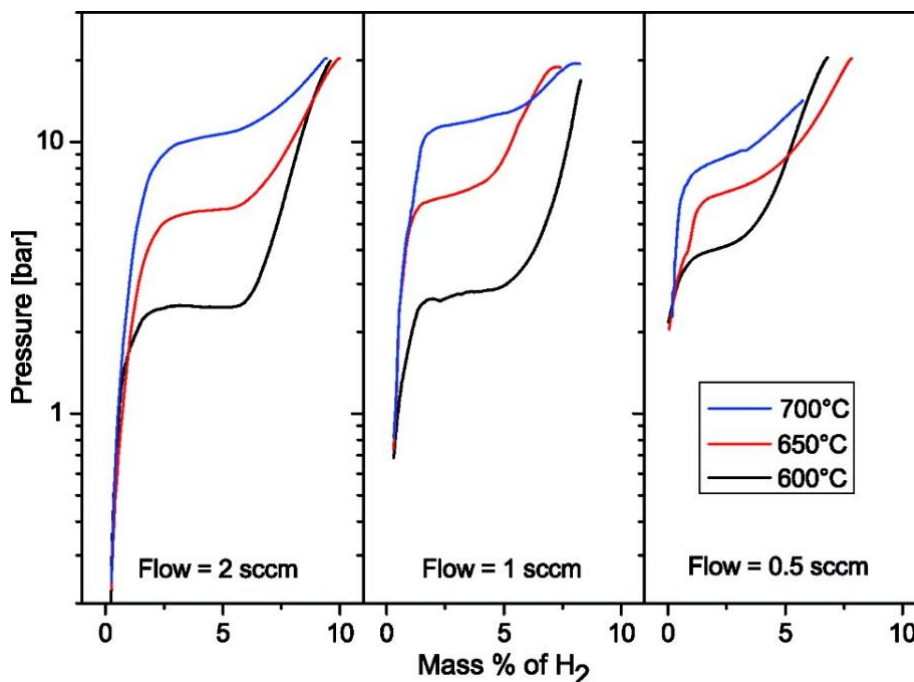
Figure 1. Pressure, composition, and temperature (PCT) isotherms measured on $NaBH_4$ at a constant hydrogen flow of 2, 1, and 0.5 cm^3 (STP) min^{-1} [7]. Reprinted with permission from [7], copyright 2010 The American Chemical Society.

Therefore, NaH is thermodynamically unstable under the decomposition conditions of $NaBH_4$ and will decompose into the corresponding elements without changing the observed equilibrium pressure. This rationalises the experimental analysis that Na is contained in the residue (as either Na or NaH). A second phase in the product was identified as either elemental boron or a boron-rich phase [7]. The Na:NaH ratio in the residue is determined by the reaction kinetics involved. The presence of traces of NaH in the product shows that $NaBH_4$ decays at least partially via NaH, which confirms the theoretical prediction [25].

Recently, the boron-containing intermediate phase $Na_2B_{12}H_{12}$ was found experimentally during the decomposition of $NaBH_4$ (and its composites). For example, Mao *et al.* [27] confirmed the formation of $Na_2B_{12}H_{12}$ by Fourier transform infrared spectroscopy (FTIR) in the decomposition of TiF_3-doped $NaBH_4$ or CaH_2-6$NaBH_4$ and $Ca(BH_4)_2$-4$NaBH_4$ composites. In contrast, Garroni *et al.* [28] detected amorphous $Na_2B_{12}H_{12}$ by nuclear magnetic resonance (NMR) in partially dehydrogenated 2$NaBH_4$-MgH_2 and in the final products of the decomposition reaction. More recently, Ngene *et al.* [29] detected $Na_2B_{12}H_{12}$ with ^{11}B solid state NMR after the dehydrogenation of a nanoconfined $NaBH_4$/porous carbon material. The formation mechanism of $Na_2B_{12}H_{12}$ is not yet clear; the borohydride may originate from the reaction of boranes with unreacted $NaBH_4$, which was proposed by the first principles calculations [25]. In fact, a similar decomposition route was proposed for $LiBH_4$, where Friedrichs *et al.* [30] suggested that the formation of $Li_2B_{12}H_{12}$ arises from the reaction of the borane evolving from $LiBH_4$ with the remaining starting material. First principles calculations suggest that $Na_2B_{12}H_{12}$ has significant ionic character and is relatively stable and if it was formed during the thermal

decomposition of $NaBH_4$, thermodynamically one would not expect its existence to be fleeting [31]. Moreover, because of its anticipated low reactivity with hydrogen, when formed it might be expected to represent a limiting step in the reverse reaction to the fully hydrogenated $NaBH_4$. In this regard, further research is required to evaluate the effects of the formation of $Na_2B_{12}H_{12}$ on both the $NaBH_4$ dehydrogenation and its subsequent re-hydrogenation.

3. Strategies for Promoting H_2 Release from Solid-State Thermolysis of $NaBH_4$

From the point where $NaBH_4$ hydrolysis was no longer considered for automotive applications by the US DOE, solid-state thermolysis has become the only realistic option for the practical use of the borohydride in hydrogen storage applications. Before this can happen, however, the kinetic and thermodynamic limitations associated with the (de)hydrogenation of $NaBH_4$ must be removed. To this end, several strategies have recently been developed and proven effective in improving the thermally activated H_2 release from $NaBH_4$ and these are considered below.

3.1. Catalytic Doping

Catalysts play an important role in the hydrogen sorption processes in hydrides, since they improve the hydrogen uptake and release kinetics by reducing the activation barrier for diffusion and facilitating hydrogen dissociation. Therefore, it is of particular interest to use catalysts to promote hydrogen exchange reactions in $NaBH_4$ under moderate temperature and pressure conditions.

Mao *et al.* [32] investigated the effects of Ti-based additives, including Ti, TiH_2, and TiF_3, on the dehydrogenation of $NaBH_4$. It was revealed that all of the titanium-based additives were effective in improving the hydrogen desorption and absorption reactions of $NaBH_4$ and among them TiF_3 possessed the highest catalytic activity (Figure 2). Powder X-ray diffraction (PXD) and X-ray photoelectron spectroscopy (XPS) revealed that the dehydrogenation of TiF_3-doped $NaBH_4$ can be regarded as a two-step process: (i) the thermodynamically-favorable reaction between borohydride and fluoride at *ca*. 300 ℃ ($3NaBH_4 + TiF_3 \rightarrow 3NaF + TiB_2 + B + 6H_2$); and (ii) the dehydrogenation of the remaining $NaBH_4$, catalysed by the NaF and TiB_2 formed *in situ* in step (i). The TiF_3-doped sample demonstrates good reversibility with *ca*. 4 wt% hydrogen absorbed below 500 ℃ at 5.5 MPa.

Ni-containing additives including Ni (20 nm), Ni_3B, $NiCl_2$, NiF_2, and Ni (65 wt%) supported on Si/Al_2O_3 reduce the dehydrogenation temperature of $NaBH_4$ by at least 60 ℃ (e.g., 65 wt% Ni on Si/Al_2O_3) [33]. PXD analysis has indicated that Ni reacts with B evolved during the thermal decomposition of $NaBH_4$ to form Ni_xB_y species including Ni_3B, Ni_2B, and Ni_3B_4. The thermodynamically favorable formation of these species is likely one reason why the dehydrogenation temperature is reduced. The reversibility is poor however and re-hydrogenation forms NaH with a maximum hydrogen uptake of *ca*. 2 wt% and no activity to hydrogenation from the additives evident. The authors also conducted a catalyst screening study of $NaBH_4$ with a variety of metal nanoparticles, chlorides, borides, and mesoporous materials. The most effective catalysis was performed by Pd nanoparticles inducing a desorption temperature of 420 ℃; a decrease of at least 85 ℃ compared to pristine $NaBH_4$. By analogy to the nickel additives above, the reduction in dehydrogenation temperature is probably enabled by the formation of Pd_xB_y intermediate phases. The reversibility of hydrogen uptake and release in the system incorporating Pd (Pd_xB_y) has yet to be reported.
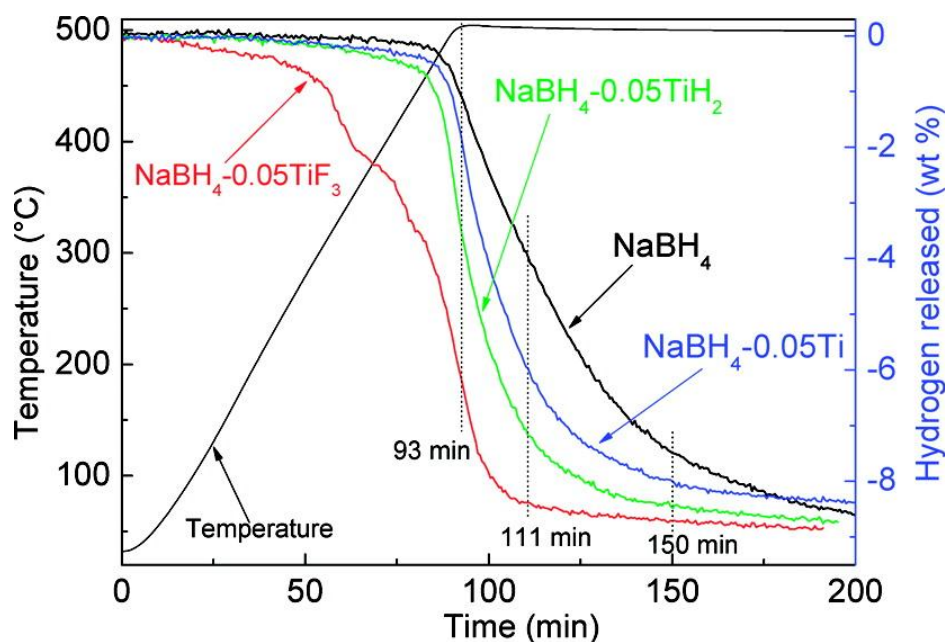
Figure 2. Temperature-programmed desorption (TPD) profiles of NaBH4 with and without different titanium catalysts. The heating rate was 5 ℃ min^{-1} [32]. Reprinted with permission from [32], copyright 2012 The American Chemical Society.

3.2. Nano-Engineering

It is well-documented that the physical and chemical properties of nanoparticles can be very different from those of the corresponding bulk materials [34]. Reducing the particle size of the metal hydride to the nanometer range can result in enhanced kinetics and in some cases, modified thermodynamics.

Metal hydride nanoparticles or nanocomposites are usually prepared by high-energy ball milling. However, the lower range of particle sizes obtained from milling is typically limited to hundreds of nanometers and the particle size distribution is usually non-uniform. For NaBH4, Varin and Chiu [35] studied the variation of the cubic lattice parameter and crystallite (grain) size with milling times of up to 200 h. It was found that the lattice parameter of the compound varies only modestly during prolonged milling (maximum ~0.15% after 50 h) and the average crystallite (grain) size remains of the order of a few tens of nanometers. Therefore, it seems that ball milling even under these relatively extreme conditions is rather limited in its ability to nanostructure NaBH4.

One sophisticated approach towards achieving genuinely nanoscale dimensions in the borohydride is to infiltrate the material into a mesoporous host matrix. Such approaches could improve the hydrogen uptake kinetics (and in some cases the thermodynamics) of hydrides significantly. Ampoumogli *et al.* [36] recently synthesized nanocomposites of NaBH4/CMK-3 (an ordered mesoporous carbon) via the impregnation of the porous carbon with NaBH4 dissolved in liquid ammonia and showed that the nanocomposite releases hydrogen at lower temperatures than bulk NaBH4. Mass spectra however, showed that the released gases contained ammonia, which could either originate from solvent that is incorporated into the pores of the carbon or form a sodium borohydride ammine complex formed during the impregnation process. In contrast, by nano-confining NaBH4 in a highly-ordered Si-based mesoporous scaffold (SBA-15) and its carbon (CMK-3) replica, respectively, through ammonia-free wet chemical impregnation, it was possible to avoid the formation of

unwanted by-products [37]. Temperature-programmed desorption (TPD) highlighted a notable reduction in dehydrogenation temperature compared to bulk NaBH$_4$, but the details of the desorption pathway, associated structural evolution and reversibility in this system are not yet clear and require further study. Recently, Ngene *et al.* [29] synthesized NaBH$_4$/C nanocomposites in which the pores of the matrix were of 2–3 nm in diameter. The materials were prepared using pore volume impregnation either with an aqueous NaBH$_4$ solution (denoted SI) or via melt infiltration (MI). It was found that each method results in a lower dehydrogenation temperature compared to pristine NaBH$_4$ [29]. The onset of hydrogen release can be reduced from 470 °C for the bulk borohydride to less than 250 °C for the nanocomposites (Figure 3). In these cases the dehydrogenated nanocomposites could be partially re-hydrogenated with the absorption of about 43% of the initial hydrogen capacity under 60 bar H$_2$ at 325 °C. The loss of capacity in this system was directly connected to partial loss of Na during dehydrogenation and this loss could be ameliorated (to retention of 98% of initial capacity) by adding further Na to the nanocomposites.
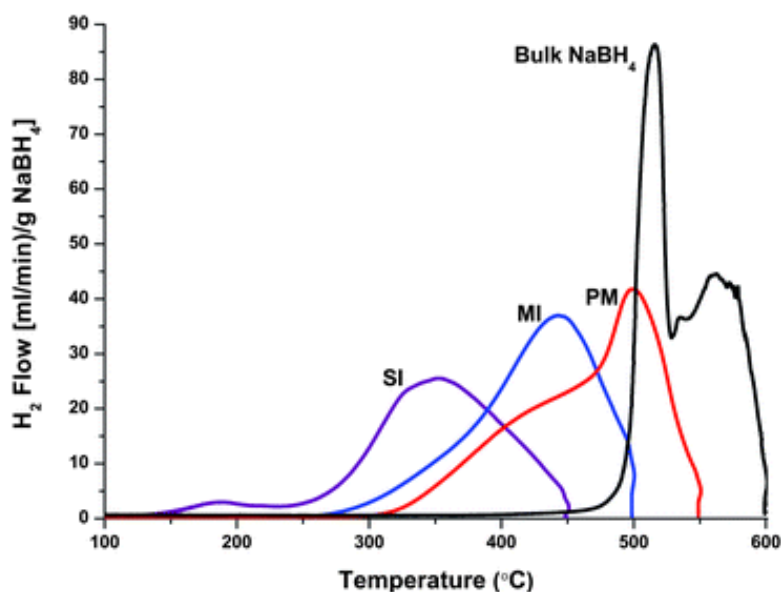
Figure 3. TPD experiments (5 °C min^{-1} under Ar) showing hydrogen release from bulk NaBH$_4$ (black); a physical mixture of 25 wt% NaBH$_4$ and porous carbon (PM; red); solution impregnated 25 wt% NaBH$_4$/C nanocomposites (SI; purple) and melt infiltration (MI; blue) 25 wt% NaBH$_4$/C nanocomposites [29]. Reproduced from [29] with permission of The Royal Society of Chemistry.

Nano-confinement in porous matrices has become a well-traveled bridge connecting bulk and nanoscale hydrogen storage materials. In addition to the unique structures and size-specific chemistry of nanomaterials, the methodology is also expected to introduce a large number of defects. Moreover, the interactions between the M–H bond and the internal surface of the nanopores may also contribute a catalytic effect to the desorption process. All these effects would promote dehydrogenation at lower temperatures. However, the weight penalty of the supporting substrates (hosts) will always reduce the gravimetric hydrogen storage capacity of the system.

In an alternative approach, Christian and Aguey-Zinsou [38,39] synthesized NaBH$_4$ nanoparticles (<30 nm in diameter) by using an anti-solvent precipitation method. The procedure resulted in a decrease of the borohydride melting point and an initial release of hydrogen at 400 °C; *ca.* 100 °C

lower than the bulk material. Encapsulation of these nanoparticles upon reaction with nickel chloride yielded core-shell nanostructures, NaBH$_4$@Ni. This core-shell material begins to release hydrogen at 50 °C with significant desorption from 350 °C. Even more remarkably, the core-shell configuration engenders full reversibility to NaBH$_4$ with hydrogen desorption/absorption occurring under 4 MPa at 350 °C (Figure 4). A consistent reversible hydrogen capacity of 5 wt% was achieved for NaBH$_4$@Ni, in which 80% of the hydrogen could be desorbed or absorbed in <60 min and full capacity could be achieved within 5 h. Although these conditions are still far from the ideal requirements for practical applications, this work suggests that the hydrogen storage performance of NaBH$_4$ can be altered dramatically by the integration of nano-engineering and catalysis concepts.
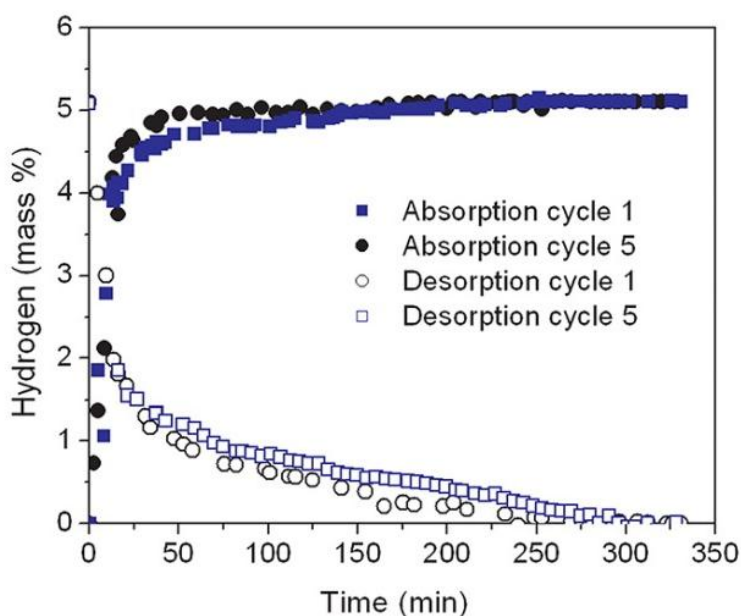
Figure 4. Kinetics of hydrogen desorption at 0.01 MPa and absorption under 4 MPa hydrogen pressure at 350 °C for NaBH$_4$@Ni [38]. Reprinted with permission from [38], copyright 2012 The American Chemical Society.

3.3. Destabilization Using Reactive Additives

Another possible way to lower the decomposition temperature of NaBH$_4$ and further tune its thermodynamic and kinetic characteristics is by the use of certain select additives. As opposed to the use of catalysts, the additive employed in these cases not only promotes the kinetics, but also tunes the thermodynamics through changing the reaction pathway. For example, the dehydrogenation thermodynamics and kinetics of NaBH$_4$ could be significantly improved by combining with fluorographite (FGi) according to the following reaction [40]:

$$x\mathrm{NaBH_4} + 4\mathrm{CF}_x \rightarrow x\mathrm{NaBF_4} + 4\mathrm{C} + 2x\mathrm{H_2} \ (x = 0.8{-}1) \tag{2}$$

The dehydrogenation onset temperature of ball-milled 55NaBH$_4$-45FGi composites can be decreased to 125 °C and approximately 4.8 wt% hydrogen can be released at 130 °C over a period of several seconds. Such additives are usually mixed with the hydrides by high-energy milling. Several additives such as hydrides and fluorides, have been found to destabilize NaBH$_4$ effectively and make the dehydrogenation or even hydrogenation possible at rather moderate pressures and temperatures.

3.3.1. Hydride Destabilization

An important potential advantage in using hydrides as a destabilizing additive over others, is that in addition to the tuning of the thermodynamics and kinetics of (de)hydrogenation, it is possible to maintain a high gravimetric capacity. For example, MgH_2 has been used successfully to modify the (de)hydrogenation thermodynamics relative to $NaBH_4$ by forming the compound MgB_2 upon dehydrogenation [41,42]. The main dehydrogenation reaction can either proceed to formation of NaH or sodium depending on the conditions:

$$2NaBH_4 + MgH_2 \rightarrow 2NaH + MgB_2 + 4H_2 \qquad 7.8 \text{ wt\%} \qquad (3)$$

$$2NaBH_4 + MgH_2 \rightarrow 2Na + MgB_2 + 5H_2 \qquad 9.8 \text{ wt\%} \qquad (4)$$
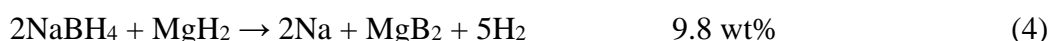
This concept is called destabilization in a "reactive hydride composite (RHC)" in which two or more hydrides are combined in appropriate ratios to lower the dehydrogenation enthalpy of the system through forming a new hydrogen-free, thermodynamically stable compound as a by-product. Hence the desorption temperature is reduced and the reversibility of the system is improved [43].

By employing this strategy, the dehydrogenation of $NaBH_4$ can be facilitated by combining the borohydride with other metal hydrides such as $LiAlH_4$, $Ca(BH_4)_2$ and CaH_2 so as to form LiAl, AlB_2 and CaB_6 respectively upon dehydrogenation [27,44]:

$$2NaBH_4 + 2LiAlH_4 \rightarrow 2Na + AlB_2 + LiAl + 8H_2 \qquad 10.6 \text{ wt\%} \qquad (5)$$

$$4NaBH_4 + Ca(BH_4)_2 \rightarrow 4Na + CaB_6 + 12H_2 \qquad 10.9 \text{ wt\%} \qquad (6)$$

$$6NaBH_4 + CaH_2 \rightarrow 6Na + CaB_6 + 13H_2 \qquad 9.7 \text{ wt\%} \qquad (7)$$

Similarly, addition of Mg_2NiH_4 to $NaBH_4$ leads to formation of the stable ternary boride phase $MgNi_{2.5}B_2$ and lowers the enthalpy of hydrogen desorption for $NaBH_4$ from 110 kJ mol^{-1} H_2 to 76 ± 5 kJ mol^{-1} H_2, according to the following reaction [45]:

$$4NaBH_4 + 5Mg_2NiH_4 \rightarrow 4NaH + 2MgNi_{2.5}B_2 + 8Mg + 16H_2 \qquad 4.5 \text{ wt\%} \qquad (8)$$
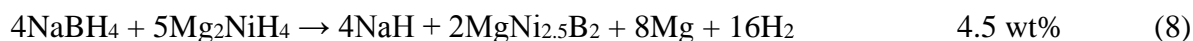
As a consequence of this addition, the onset temperature of hydrogen desorption decreases from *ca*. 500 °C for $NaBH_4$ to 360 °C for the $NaBH_4/Mg_2NiH_4$ composite mixture. When Mg_2FeH_6 is added to $NaBH_4$ the dehydrogenation can become quite complex [46]. A single dehydriding step is observed for $xNaBH_4 + (1-x)Mg_2FeH_6$ when $x = 0.1$ and 0.125, but a multi-step process occurs when $x > 0.25$. Despite the different dehydriding process, PXD measurements maintain that NaH and MgB_2 are the dehydrogenation products over the entire composition range. The results also indicate that the dehydriding temperature of $NaBH_4$ is reduced by at least 150 °C when combined with Mg_2FeH_6.

As a model borohydride-hydride system, the $NaBH_4$-MgH_2 combination has been investigated extensively. For $2NaBH_4 + MgH_2$, the dehydrogenation temperature is reduced by *ca*. 40 °C compared to pure $NaBH_4$ [41]. The desorption was originally proposed to follow a two-step process:

$$2NaBH_4 + MgH_2 \rightarrow 2NaBH_4 + Mg + H_2 \qquad (9)$$

$$\rightarrow 2NaH + MgB_2 + 4H_2 \qquad (10)$$
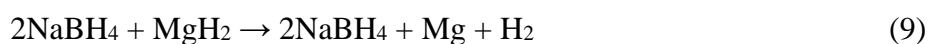
The dehydriding mechanism of the $2NaBH_4 + MgH_2$ system was subsequently suggested to proceed in three steps under 1 bar of inert gas, by: (i) the dehydrogenation of MgH_2; (ii) the "disproportion"

of $NaBH_4$; and (iii) the reaction of an intermediate borohydride compound, such as $Na_2B_{12}H_{12}$, with free Mg to give MgB_2, NaH and hydrogen [42,47]:

$$2NaBH_4 + MgH_2 \rightarrow Mg + H_2 + 2NaBH_4 \tag{11}$$

$$\rightarrow 1/6Na_2B_{12}H_{12} + 5/3NaH + Mg + 19/6H_2 \tag{12}$$

$$\rightarrow 2NaH + MgB_2 + 4H_2 \tag{13}$$

However, no direct observation of $Na_2B_{12}H_{12}$ was made. When the reaction is performed under static vacuum, however, the dehydrogenation of $2NaBH_4$-MgH_2 appears to follow an alternative pathway (Figure 5) [48]:

$$2NaBH_4 + MgH_2 \rightarrow 2NaBH_4 + 1/2MgH_2 + 1/2Mg + 1/2H_2 \tag{14}$$

$$\rightarrow 3/2NaBH_4 + 1/4MgB_2 + 1/2NaH + 3/4Mg + 7/4H_2 \tag{15}$$

$$\rightarrow 2Na + B + 1/2Mg + 1/2MgB_2 + 5H_2 \tag{16}$$
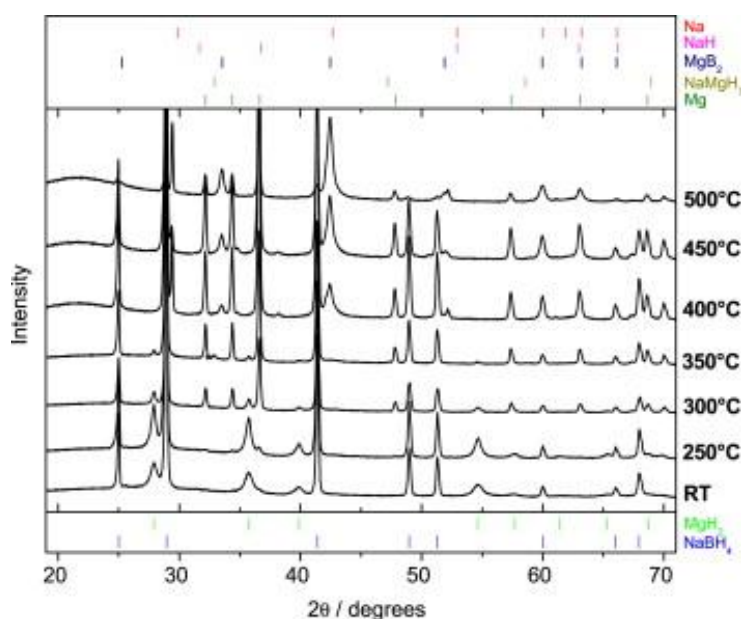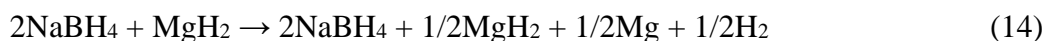
Figure 5. Powder X-ray diffraction (PXD) patterns of $2NaBH_4$-MgH_2 with increasing temperature [48]. Reprinted from [48] with permission from the International Association of Hydrogen Energy.

The presence of the $B_{12}H_{12}^{2-}$ anion was confirmed experimentally by solid state NMR. Amorphous $Na_2B_{12}H_{12}$ was detected in a partially desorbed $2NaBH_4 + MgH_2$ sample (following 2 h at 450 °C) and in the final products of the decomposition reaction by both direct comparison with the $^{11}B\{^{1}H\}$ NMR spectrum of pure $Na_2B_{12}H_{12}$ and by dynamic cross-polarization experiments [28].

Considering now the reverse hydrogenation reaction in the Na-Mg-B-H system, it has been suggested that the hydrogenation of $2NaH$-MgB_2 proceeds according to the following reaction [41]:

$$2NaH + MgB_2 + 4H_2 \rightarrow 2NaBH_4 + MgH_2 \tag{17}$$

Further scrutiny of the process indicated that the absorption reaction does not occur in a single step. Nwakwuo *et al.* [49] and Pistidda *et al.* [50], respectively, characterized the uptake mechanism of

ball-milled 2NaH-MgB$_2$ by using transmission electron microscopy (TEM) and *in situ* PXD. Under 50 bar of hydrogen, a new and unknown hydride phase was observed at *ca.* 280 °C. This phase remained present in diffraction patterns up to 325 °C followed by the formation of NaMgH$_3$ at about 330 °C. At 380 °C, crystals of NaBH$_4$ appeared and grew (Figure 6). The effect of the NaH:MgB$_2$ ratio on hydrogen uptake in the system has since become evident [51]. Unlike the 2:1 NaH:MgB$_2$ hydrogenation reaction, the only crystalline products of the hydrogenation of the 1:1 and 1:2 mixtures are NaBH$_4$ and MgH$_2$. Due to the reduced amount of NaH in the 1:2 system, the hydrogenation reaction proceeds towards the formation of NaBH$_4$ and MgH$_2$, completely consuming the NaMgH$_3$ formed and avoiding the formation of a molten NaH-NaBH$_4$ phase.
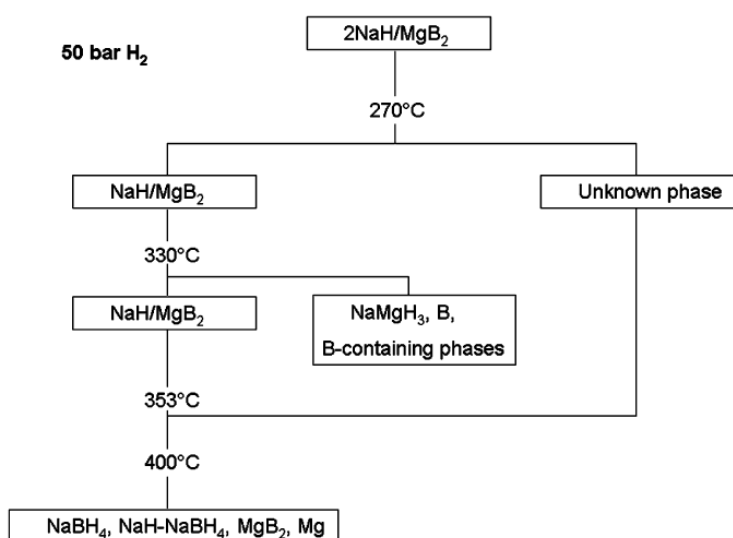
Figure 6. Scheme of the 2NaH + MgB$_2$ absorption reaction performed under 50 bar H$_2$ [50]. Reprinted with permission from [50], copyright 2010 The American Chemical Society.

NaBH$_4$ can also be synthesized from NaH and MgB$_2$ under hydrogen by mechanochemical methods, but only partial hydrogenation is observed [52]. Although the formation of NaBH$_4$ was experimentally observed by *ex-situ* [11]B magic angle spinning (MAS) NMR under 1 bar of H$_2$ with a milling speed of 300 rpm, even at 120 bar H$_2$/550 rpm the yield of NaBH$_4$ was only 14 wt% (by PXD). Moreover, IR spectroscopy confirmed MgH$_2$ in the milling products.

Hence, the above examples demonstrate that the dehydrogenation thermodynamics of NaBH$_4$ are significantly improved by adding MgH$_2$ and that re-hydrogenation is possible. To obtain improvements in release kinetics and/or achieve dehydrogenation temperatures below 400 °C, approaches such as catalytic doping and nanoconfinement have been attempted for the Na-Mg-B-H system just as with NaBH$_4$ itself. 5 mol% TiF$_3$ doping reduces the dehydrogenation temperature of the 2NaBH$_4$-MgH$_2$ system by 100 °C [41]. Moreover, TiF$_3$ doped 2NaBH$_4$-MgH$_2$ can be rehydrogenated up to 5.89 wt% hydrogen within 12 h at 600 °C and 4 MPa H$_2$. NaBH$_4$ and MgH$_2$ are the clearly observed re-hydrogenation products by PXD. Of several other additives (fluorides, chlorides and hydroxides), the most promising would appear to be MgF$_2$ [8]. The MgF$_2$ reduces the NaBH$_4$ decomposition temperature by 30 °C and the desorption enthalpy by 2 kJ mol^{-1}. The rate constant for desorption (fitted to a modified Avrami-Erofeev equation over the isothermal region) increases by a factor of 3.2 when MgF$_2$ is added.

Perhaps rather unexpectedly, short-term exposure to a moist atmosphere appears to have a positive effect on the desorption reaction of the $2NaBH_4 + MgH_2$ mixture [53]. The as-milled mixture desorbs 3.4 wt% of hydrogen at 450 °C, whereas 7.8 wt% of hydrogen is desorbed from the milled sample after 2 h of air exposure followed by drying. In this latter case, the final products are MgB_2 and NaH (in addition to some NaOH) whereas in the former, partial dehydrogenation yields $NaBH_4$ and Mg. Further investigation showed that the chemical state of the reactants is unchanged after exposure, but significant microstructural and morphological differences were revealed by Rietveld analysis and scanning electron microscope (SEM) characterization of the starting materials. It seems that the exposure of the 2:1 $NaBH_4$:MgH_2 system to moisture creates a scenario where the MgH_2 remains solid whereas the $NaBH_4$ forms a slurry that "wets" the surface of the MgH_2 particles (protecting the MgH_2 from reaction with air). The intimate interfacial contact is maintained in the solid state during the subsequent drying procedure facilitating dehydrogenation.

The effects of nanoconfinement have been evaluated against physically nanostructured mixtures by melt infiltration of $NaBH_4$-MgH_2 into mesoporous SBA-15 (NbF_5 was used as a catalyst in both cases) [54]. The thermal desorption profile of $2NaBH_4 + MgH_2$ shows two peaks at *ca.* 300 °C and 410 °C, respectively. When 0.05 mol of NbF_5 is added, the desorption profile of the mixture displays three peaks centered at *ca.* 200 °C, 300 °C, and 400 °C, respectively. The comparison of the two traces suggests that the NbF_5 additive actively alters the dehydrogenation process in the $2NaBH_4 + MgH_2$ system. If the same hydrides are nanoconfined ($2NaBH_4 + MgH_2 + 0.05$ mol NbF_5 confined into SBA-15), three desorption peaks occur at 134 °C, 323 °C and 354 °C, respectively. The changes in the desorption temperatures suggests that different reaction processes again occur in the nanoconfined-catalyzed material. Although Si-containing phases in the dehydrogenation product suggest that SBA-15 cannot be treated as an inert host, only hydrogen is observed as an evolved gas. The results indicate that favorable synergic effects between nanoconfinement and catalysis may exist for the Na-Mg-B-H system as have been observed for $NaBH_4$ itself. The reasons for these phenomena require further investigation.

3.3.2. Fluoride Destabilization

Despite improvements in performance over pristine $NaBH_4$, destabilized systems such as those in Section 3.3.1 have been unable to achieve gravimetric hydrogen capacities on a level with theoretical maxima. Given that the melting point of the decomposition product, Na, is ~371 K [55] and that molten Na may serve as an effective mass-transfer medium to promote atomic/ionic diffusion, one possible reason for this under-performance in the Na-Mg-B-H system is that a melting-induced phenomenon takes place during dehydrogenation. As a result, the local stoichiometry and homogeneity of the mixture may be disrupted, hindering rehydrogenation to $NaBH_4$. Alternatively, hydrogen released during dehydrogenation may transport Na away from the reaction mixture in the liquid and/or vapor phase. To prevent such eventualities, Na may be confined to the solid state (together with boron) by using certain additives such as metal fluorides. On the one hand, boron, the decomposition product of $NaBH_4$ can be stabilized by other metals to form borides while on the other, Na forms NaF with a significantly elevated melting point compared to Na metal (*i.e.*, a more than 3-fold increase; 1263 K) [56].

In addition, and also important, the thermodynamic and kinetic behaviour of $NaBH_4$ dehydrogenation itself may be tuned through the substitution of fluorine for hydrogen since H^- and F^- have similar

ionic radii [57]. For example, a recent study on the $NaBH_4$–$NaBF_4$ system showed that hydrogen–fluorine exchange took place in a temperature range of 200–215 °C, leading to a new rock salt-type compound with idealized composition $NaBF_2H_2$ [58]. After further heating, the fluorine substituted compound becomes X-ray amorphous and decomposes to NaF at 310 °C. In particular, the $NaBH_4$–$NaBF_4$ composite decomposes at lower temperatures ($T = 300$ °C) compared to $NaBH_4$ ($T = 476$ °C) and retains 30% of the hydrogen storage capacity after three hydrogen release and uptake cycles compared to 6% for $NaBH_4$.

Two new systems based on $2NaF + MgB_2 + 0.05TiF_3$ (referred to here as the "Mg system") and $2NaF + AlB_2 + 0.05TiF_3$ ("Al system") were investigated by employing a fluorine-hydrogen substitution strategy [59]. The hydrogenation of the Mg system yielded $NaBH_4$ and MgF_2, which can be dehydrogenated to $NaMgF_3$ and MgB_2. In contrast, the hydrogenation of the Al system yielded $NaBH_4$ and Na_3AlF_6, which was dehydrogenated to NaF and AlB_2. These processes are therefore reversible and compared to pure $NaBH_4$ a significant kinetic and thermodynamic destabilisation with respect to the hydrogenation and dehydrogenation is achieved (Figure 7). The reversible hydrogen storage capacity reached 3.8 wt% and 2.5 wt% for the Mg and Al systems, respectively.
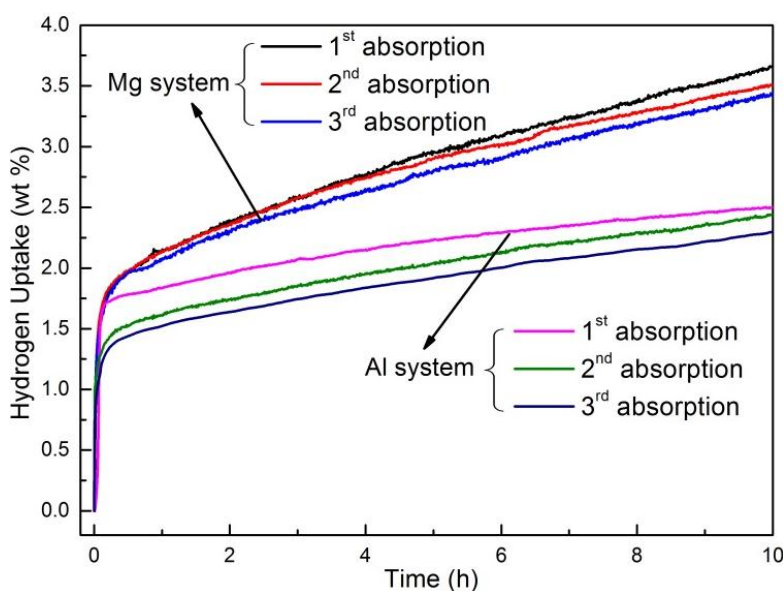
Figure 7. Hydrogenation and dehydrogenation curves for the $2NaF$–MgB_2 (AlB_2)–$0.05TiF_3$ systems on cycling at 500 °C and 6 MPa hydrogen pressure [59]. Reproduced from [59] by permission of The Royal Society of Chemistry.

Combining $NaBH_4$ and ZnF_2 generates hydrogen by forming $NaBF_4$ with an onset temperature below 100 °C with favorable kinetics [60]. However, a small amount of B_2H_6 is released and the reversibility of the system is unknown. Studies of the effect of transition metal fluorides on the decomposition of $NaBH_4$ by reacting $NaBH_4$ with TiF_3 mechanochemically, MnF_3 or FeF_3 revealed that $NaBF_4$ was among the products in all cases [61]. Analysis of ^{11}B-NMR spectra gave $NaBF_4$:$NaBH_4$ ratios of 1:150, 1:40 and 1:10 for the Ti-, Mn- and Fe-containing systems respectively. The hydrogen release in the $NaBH_4$–MnF_3 system began at 130 °C while FeF_3 decreased the onset temperature to 161 °C and TiF_3 to 200 °C. TiF_3 reacted completely with $NaBH_4$ below 320 °C. All these 3d transition metal fluoride containing materials display negligible emissions of diborane species.

Both dehydrogenation and hydrogenation can be improved by adding rare earth fluorides (LnF_3, Ln = Nd, Y, La, Ho) [62–65]. The 3 $NaBH_4$/LnF_3 composites release hydrogen between 400 °C and 450 °C, which is lower than that of pure $NaBH_4$. Approximately 3 wt% hydrogen can be cycled in these systems. By analogy to the destabilization mechanisms proposed for other metal fluoride "composite" systems, the improvement can be attributed to the formation of borides according to the following reactions:

$$LnF_3 + 3NaBH_4 \rightarrow 3NaF + 3/xLnB_x + (1 - 3/x)LnH_y + (12 - y + 3y/x)/2H_2 \qquad (18)$$
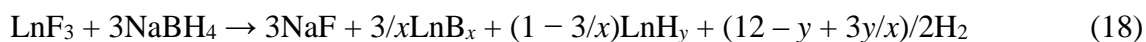
For example, dehydrogenation commences at 413 °C under 0.1 MPa Ar for the 3$NaBH_4$/NdF_3 system [62]. PXD revealed that NdB_6, Nd_2H_5 and NaF formed on decomposition. The process is pseudo-reversible, producing $NaBH_4$ and $NaNdF_4$ on hydrogenation. Similarly, dehydrogenation of 3$NaBH_4$/YF_3 starts at 423 °C but with a higher mass loss of 4.12 wt% (given the lower atomic mass of Y over Nd) [63]. PXD of the dehydrogenated products reveals NaF, YB_4 and YH_2 are formed and re-hydrogenation leads to $NaBH_4$ and $NaYF_4$ by analogy to the neodymium system.

The above shows that the products from $NaBH_4$ dehydrogenation can be stabilized simultaneously by introducing both fluorine and metals, hence effectively destabilizing $NaBH_4$. Although the conditions required for dehydrogenation and rehydrogenation in these systems are still too extreme for practical applications, the improvement in uptake and release provides the basis for a broader destabilization strategy.

3.4. Chemical Modification

3.4.1. Combination of Protic and Hydridic H Atoms

It is well known that hydrogen exists in a partially negatively charged state ($H^{\delta-}$) in complex hydrides such as $NaBH_4$, whereas it is partially positively charged ($H^{\delta+}$) in nitrogen containing compounds such as $LiNH_2$. Given the repulsive potential between two positively charged ($H^{\delta+}$/$H^{\delta+}$) or two negatively charged ($H^{\delta-}$/$H^{\delta-}$) species, there are relatively high energy barriers to the conversion of either $H^{\delta-}$ or $H^{\delta+}$ pairs to neutral H_2. This contrasts markedly with the ease of combining $H^{\delta-}$ and $H^{\delta+}$ [66]. These observations suggest that the reaction kinetics of H_2 formation can be enhanced by inducing H^+ and H^- mobility in compounds with suitable structures. Thus, it is of particular interest to consider the range of $H^{\delta+}$-rich compounds that could be combined with $NaBH_4$ to improve dehydrogenation.

Chater *et al.* [67] found a new cubic phase in the $NaNH_2$–$NaBH_4$ system with composition Na_2BNH_6 ($a \approx 4.7$ Å) at 190 °C. Hydrogen release initiates at *ca*. 290 °C in Na_2BNH_6 and peaks at ~350 °C. Ammonia is also released, constituting approximately 7 wt% of the total desorbed gas. The decomposition products are reported to be NaH, Na and an amorphous unidentified white solid. In fact, Na_2BNH_6 releases hydrogen while molten between 300 °C and 400 °C yielding NaH, Na and a grey amorphous powder [68]. On addition of excess amide (≥2:1 $NaNH_2$:$NaBH_4$), Na_3BN_2 becomes the sole product.

Another new phase in the $NaNH_2$–$NaBH_4$ system, $Na_3(NH_2)_2BH_4$, is attainable by ball milling (at a molar ratio of 2:1) [69]. Thermal analysis shows that decomposition occurs in two main stages: (i) dehydrogenation below 400 °C to form Na_3BN_2 (6.85 wt%); and (ii) decomposition of Na_3BN_2 above 400 °C to produce Na, B, and N_2 according to the following reactions:

$$Na_3(NH_2)_2BH_4 \rightarrow Na_3BN_2 + 4H_2 \rightarrow 3Na + B + N_2 + 4H_2 \qquad (19)$$

Another example in terms of "protic" species that could be combined with borohydrides, is that of hydroxide. Drozd *et al.* [70] investigated the hydrogen-generating reaction between $NaBH_4$ and $Mg(OH)_2$, and found that reaction rate depends tremendously on the homogeneity and/or particle size of the reactants. PXD and Raman spectroscopy reveal that mechanically activated mixtures of $NaBH_4$ and $Mg(OH)_2$ react yielding MgO as the only crystalline phase between 240 ℃ and 318 ℃. Ball milled $NaBH_4$-$2Mg(OH)_2$ mixtures release hydrogen in one exothermic reaction, with an onset temperature of 240 ℃ [71]. The estimated enthalpy for the reaction is 135.9 kJ mol^{-1} and the dehydrogenation products contain $NaBO_2$ and MgO [70]. Therefore, the following dehydrogenation reaction was proposed:

$$NaBH_4 + 2Mg(OH)_2 \rightarrow NaBO_2 + 2MgO + 4H_2 \qquad 5.18 \text{ wt\%}; \, \Delta H = -135.9 \text{ kJ mol}^{-1} \qquad (20)$$
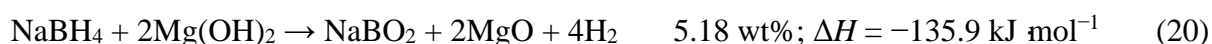
The various studies above show that the dehydrogenation of $NaBH_4$ can be improved by reaction with $H^{\delta+}$-containing starting materials (such as $NaNH_2$ or $Mg(OH)_2$) based on the premise of favorable H^+-H^- interactions. However, the dehydrogenation reaction of these systems can be exothermic, which clearly introduces substantial challenges in terms of cycling or regeneration.

3.4.2. Bimetallic Borohydrides

Nakamori *et al.* [72,73] theoretically and experimentally found that a clear correlation exists between the thermodynamic stability of metal borohydrides and the Pauling electronegativity of the respective metal cations (Figure 8). It was thus proposed that the dehydrogenation temperature of $M(BH_4)_n$, where M is a metal cation of valence *n*, decreases linearly with the increasing electronegativity of M. Hence one of the approaches to adjust the dehydrogenation thermodynamics of metal borohydrides is to substitute an alkali or alkaline earth metal, for example, by another metal with higher electronegativity.
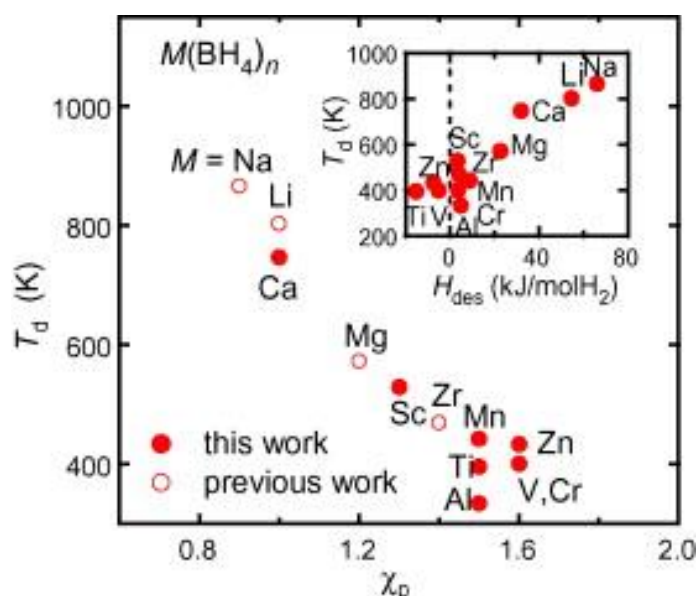
Figure 8. The dehydrogenation temperature, T_d as a function of the Pauling electronegativity χ_p for selected metals. The inset shows the correlation between T_d and estimated H_{des} for the desorption reaction [73]. Reprinted with permission from [73], copyright 2007 Elsevier.

NaK(BH$_4$)$_2$ was synthesized by mechanical milling of NaBH$_4$ and KBH$_4$ in a 1:1 ratio [74]. The new phase forms with a rhombohedral structure (tentatively space group *R*3), but *in situ* PXD indicated it was metastable, decomposing to the starting materials NaBH$_4$ and KBH$_4$ after 14 h at room temperature. A more common method for the synthesis of bimetallic sodium borohydrides is by solid or solution-state metathesis [75]:

$$x\text{NaBH}_4 + \text{MCl}_y \rightarrow \text{Na}_{x-y}\text{M(BH}_4)_x + y\text{NaCl} \tag{21}$$
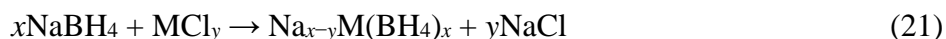
where M is an alkali metal, alkaline earth metal, transition metal or lanthanide. For example, the new bimetallic borohydride NaSc(BH$_4$)$_4$ was synthesised by ball-milling mixtures of sodium borohydride and ScCl$_3$ [76]. The structure of NaSc(BH$_4$)$_4$ (orthorhombic space group *Cmcm* a = 8.170(2) Å, b = 11.875(3) Å, c = 9.018(2) Å) consists of isolated scandium tetraborohydride tetrahedral anions, [Sc(BH$_4$)$_4$]$^-$, located inside slightly distorted trigonal Na$_6$ prisms (each second prism is empty) (Figure 9). Na$^+$ is surrounded by six BH$_4^-$ tetrahedra in almost regular octahedral coordination with a (6 + 12)-fold coordination of H to Na. NaSc(BH$_4$)$_4$ melts at ~137 ℃ subsequently releasing hydrogen in two steps between 167–217 ℃ and 222–267 ℃. Scandium boride ScB$_x$ is tentatively identified as one of the decomposition products.
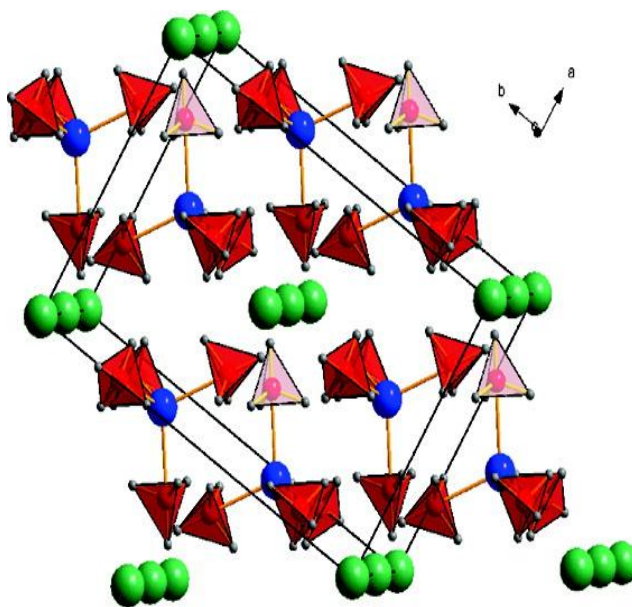
Figure 9. Crystal structure of NaSc(BH$_4$)$_4$ showing the coordination of Sc atoms (blue) by BH$_4$ tetrahedra (red); Na atoms are in green [76]. Reprinted with permission from [76], copyright 2010 The American Chemical Society.

NaZn(BH$_4$)$_3$ can be synthesized by ball milling NaBH$_4$ and ZnCl$_2$ in a 3:1 molar ratio and in fact if the starting ratios are varied (e.g., 2:1, 4:1) mixtures of NaZn$_2$(BH$_4$)$_5$ and NaZn(BH$_4$)$_3$ are obtained, indicating competitive reactions [77]. NaZn(BH$_4$)$_3$ (monoclinic space group *P*2$_1$/*c*; Figure 10) consists of 1D anionic [{Zn(BH$_4$)$_3$}$_n$]$^{n-}$ chains with tetrahedrally coordinated Zn atoms, which are connected in three dimensions through the Na$^+$ ions. NaZn$_2$(BH$_4$)$_5$ meanwhile, is unstable and slowly decomposes to NaZn(BH$_4$)$_3$ at room temperature. The structure of NaZn$_2$(BH$_4$)$_5$ (also monoclinic space group *P*2$_1$/*c*) consists of Na$^+$ cations and isolated complex dimeric [Zn$_2$(BH$_4$)$_5$]$^-$ anions in which trigonal planar centers of Zn are each coordinated to one bridging and two terminal BH$_4$ groups.
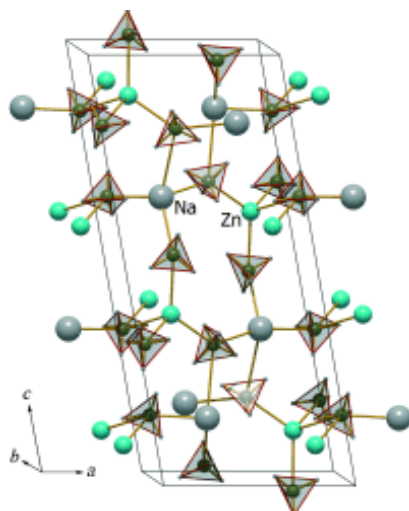
Figure 10. Crystal structure of NaZn(BH$_4$)$_3$; Zn atoms in blue, B in brown, Na in dark grey, and H in light grey [77]. Reprinted with permission from [77], copyright 2009 John Wiley & Sons.

Pure NaZn(BH$_4$)$_3$, synthesized by a solution route, releases hydrogen coupled with borane and diborane BH$_3$, and B$_2$H$_6$, giving a total weight loss of 29 wt% between 80 °C and 200 °C [78]. Nanoconfinement of NaZn(BH$_4$)$_3$ in SBA-15 however leads to borane-free hydrogen evolution across a temperature range of 50–150 °C from onset to completion. The activation energy for dehydrogenation was reduced to 38.9 kJ·mol^{-1} in the nanoconfined solid; a reduction of 5.3 kJ·mol^{-1} compared to that of bulk NaZn(BH$_4$)$_3$.

The novel mixed-cation mixed-anion borohydride chloride, NaY(BH$_4$)$_2$Cl$_2$ was prepared by mechanochemical synthesis from NaBH$_4$-YCl$_3$ mixtures followed by annealing (with Na$_3$YCl$_6$ and Na(BH$_4$)$_{1-x}$Cl$_x$ as impurity phases) [79]. The structure of NaY(BH$_4$)$_2$Cl$_2$ is pseudo-orthorhombic (monoclinic space group *P*2/*c*) and isotypic with the high temperature polymorph of NaYCl$_4$. The borohydride chloride is comprised of edge- and corner-sharing yttrium-centered and sodium-centered octahedra (Y is coordinated by four Cl and two BH$_4$ ligands, whereas Na is coordinated by two Cl and four BH$_4$ ligands; Figure 11).
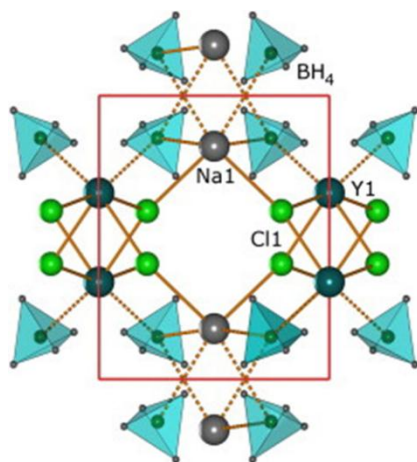
Figure 11. Crystal structure of NaY(BH$_4$)$_2$Cl$_2$ at *T* ~ 230 °C [79]. Reprinted from [79] with permission from the International Association of Hydrogen Energy.

In situ synchrotron PXD studies show that NaY(BH$_4$)$_2$Cl$_2$ decomposes to Na$_3$YCl$_6$ with amorphous yttrium borides the likely other products. The decomposition is an endothermic process that occurs at *ca*. 300 °C and the observed thermogravimetric analysis (TGA) mass losses suggest that no significant amount of diborane is released during the decomposition.

The thermal decomposition of ball milled mixtures of NaBH$_4$ with the chlorides of the 3d transition metals and cadmium (M) has been systematically investigated (Table 2) [75]. In contrast to predictions from theory, which in many cases have suggested the formation of mixed metal borohydrides [80], all the above reactions involve the substitution of BH$_4^-$ by Cl$^-$ and the formation of cubic NaCl-type Na(BH$_4$)$_{1-x}$Cl$_x$ solid solutions (with presumed amorphous transition metal borides as the other product in most cases). Samples containing Sc, Mn and Zn release <0.05 mol gas per mol of Na atoms during milling whereas the remainder of the 3d transition metal samples release *ca*. 1 mol of gas per mol of Na atoms with Fe- and Co-containing samples reaching maximum gas release most quickly (after 1 h).

Table 2. Structural and thermal decomposition parameters for ball milled NaBH$_4$ + MCl$_n$ powders (mixed in in 3:1 (MCl$_2$) or 4:1 (MCl$_3$) ratios). Note: the parameters for M = Sc were not reported [75]. Reprinted from [75] with permission from Elsevier; copyright 2012.

Starting reagents	Na(BH$_4$)$_{1-x}$Cl$_x$ cell parameter, *a*/Å	Cl content, *x*	Decomposition *T*/ °C	Mass loss at *T* ≤ 600 °C/wt%
NaCl only	5.6400(5)	1	-	-
NaBH$_4$/TiCl$_2$	5.7685(3)	0.71	401	2.7
NaBH$_4$/VCl$_3$	5.7306(4)	0.79	391	3.0
NaBH$_4$/CrCl$_3$	5.7383(2)	0.77	397	-
NaBH$_4$/MnCl$_2$	5.7863(4)	0.68	146	5.7
NaBH$_4$/FeCl$_3$	5.7407(4)	0.77	397	0.2
NaBH$_4$/CoCl$_2$	5.8011(3)	0.65	413	3.6
NaBH$_4$/NiCl$_2$	5.7837(9)	0.68	391	4.0
NaBH$_4$/CuCl$_2$	5.7801(3)	0.69	343	3.7
NaBH$_4$/ZnCl$_2$	5.6576(2)	0.92	103	21.7
NaBH$_4$/CdCl$_2$	5.7572(8)	0.74	521	-
NaBH$_4$ only	6.13080(10)	0	-	-

In subsequent thermal desorption experiments, the maximum release temperature ranges from 103 °C (Zn) to 521 °C (Cd) and NaBH$_4$–NaCl samples demonstrate decomposition at *ca*. 500 °C, similar to pure NaBH$_4$. That Sc, Mn, and Zn form other stable compounds in addition to Na(BH$_4$)$_{1-x}$Cl$_x$ (e.g., NaZn(BH$_4$)$_3$ which decomposes between 92 °C and 112 °C) explains the low decomposition temperatures observed (*i.e.*, below 230 °C). In fact, the trends in decomposition temperatures can be related to these compounds and to kinetic effects rather than to a systematic destabilisation of the NaBH$_4$ cubic structure. V, Ni and Ti, for example, form borides, which can act as catalysts whereas for Cu and Cd the high desorption temperatures would indicate the presence of metallic Cd and Cu, which have no beneficial effect on decomposition.

4. Closing Remarks

NaBH$_4$ is undoubtedly a very interesting material for hydrogen storage due to its high hydrogen density (10.6 wt%), low cost and relative air stability. However, the high dehydrogenation temperature,

slow kinetics and poor reversibility are challenges that have to be overcome before the borohydride could be considered for practical applications. Several approaches to tackle both thermodynamic and kinetic issues have been employed ranging from catalysis through nano-engineering and additive destabilization to chemical modification. From the discussions in the sections above, it is apparent that each input can make a successful impact in terms of modifying thermodynamic stability, reducing dehydrogenation temperatures, improving equilibrium pressures, lowering activation energies or optimizing reversible capacity. While sorption kinetics can be enhanced, catalysis alone is not capable of altering the thermodynamics of uptake and release and hence reversibility. Various chemical destabilization, doping and "composite" approaches confront these issues via creating alternative reaction pathways for uptake and release. These strategies can either increase of decrease gravimetric capacity depending on the "activity" of the added components to making (and breaking) bonds with hydrogen. So-called nano-engineering methods such as nanoconfinement or the formation of core-shell nanostructures can combine the benefits of catalysis and chemical modification, but often to the detriment of gravimetric capacity. The benefits and drawbacks of each approach relative to the hydrogen storage performance of $NaBH_4$ itself are summarized in Table 3.

Table 3. Comparison of materials modification approaches relative to $NaBH_4$ itself (where "+" signifies an improvement and "−" signifies a decline).

Strategy	T_d [a]	Kinetics	wt% H_2 [b]	Cyclability	References
Catalytic doping	+	+	−	+	[32,33]
Nano-confinement	+	+	−	+	[29,36–39]
H^- destabilisation	+	+	+	+	[27,41–45]
F^- destabilisation	+	+	−	+	[40,59–65]
$H^{\delta+}$-$H^{\delta-}$ "composites"	+	+	−	−	[66–71]
Bimetallic Na borohydrides	+	+	−	−	[74–80]

[a] Dehydrogenation onset temperature; and [b] practically realizable gravimetric capacity.

Clearly, all these strategies demonstrably help overcome one or more of the limitations of pristine $NaBH_4$ as a thermally-driven hydrogen store, but thus far, no modified materials can simultaneously meet all the major performance criteria required for mobile applications. The screening of more suitable catalysts and additives, developing new techniques to fabricate nanomaterials, discovering suitable lightweight mesoporous hosts, restricting loss of molten Na and greater understanding of the mechanisms involved in hydrogen release and uptake are some of the principal objectives towards making $NaBH_4$-based systems viable. However, it may be a radically different approach in which $NaBH_4$ is a component part that finally delivers a practical solution.

Acknowledgments

Conflicts of Interest

The authors declare no conflict of interest.

References

1. Schlapbach, L.; Züttel, A. Hydrogen-storage materials for mobile applications. *Nature* **2001**, *414*, 353–358.
2. Eberle, U.; Felderhoff, M.; Schüth, F. Chemical and physical solutions for hydrogen storage. *Angew. Chem. Int. Ed.* **2009**, *48*, 6608–6630.
3. Yang, J.; Sudik, A.; Wolverton, C.; Siegel, D.J. High capacity hydrogen storage materials: Attributes for automotive applications and techniques for materials discovery. *Chem. Soc. Rev.* **2010**, *39*, 656–675.
4. Reardon, H.; Hanlon, J.M.; Hughes, R.W.; Godula-Jopek, A.; Mandal, T.K.; Gregory, D.H. Emerging concepts in solid-state hydrogen storage the role of nanomaterials design. *Energy Environ. Sci.* **2012**, *5*, 5951–5979.
5. U.S. Department of Energy, Office of Energy Efficiency and Renewable Energy and the FreedomCAR and Fuel Partnership. Technical System Targets: Onboard Hydrogen Storage for Light-Duty Fuel Cell Vehicles. Available online: http://energy.gov/sites/prod/files/2014/03/f12/targets_onboard_hydro_storage.pdf (accessed on 23 December 2014).
6. Urgnani, J.; Torres, F.J.; Palumbo, M.; Baricco, M. Hydrogen release from solid state $NaBH_4$. *Int. J. Hydrog. Energy* **2008**, *33*, 3111–3115.
7. Martelli, P.; Caputo, R.; Remhof, A.; Mauron, P.; Borgschulte, A.; Züttel, A. Stability and decomposition of $NaBH_4$. *J. Phys. Chem. C* **2010**, *114*, 7173–7177.
8. Milanese, C.; Garroni, S.; Girella, A.; Mulas, G.; Berbenni, V.; Bruni, G.; Suriach, S.; Baró, M.D.; Marini, A. Thermodynamic and kinetic investigations on pure and doped $NaBH_4$-MgH_2 system. *J. Phys. Chem. C* **2011**, *115*, 3151–3162.
9. Züttel, A.; Rentsch, S.; Fischer, P.; Wenger, P.; Sudan, P.; Mauron, P.; Emmenegger, C. Hydrogen storage properties of $LiBH_4$. *J. Alloys Compd.* **2003**, *356–357*, 515–520.
10. Mao, J.F.; Guo, Z.P.; Liu, H.K.; Yu, X.B. Reversible hydrogen storage in titanium-catalyzed $LiAlH_4$–$LiBH_4$ system. *J. Alloys Compd.* **2009**, *487*, 434–438.
11. Mauron, P.; Buchter, F.; Friedrichs, O.; Remhof, A.; Bielmann, M.; Christoph, N.Z.; Züttel, A. Stability and reversibility of $LiBH_4$. *J. Phys. Chem. B* **2008**, *112*, 906–910.
12. Yu, X.B.; Grant, D.M.; Walker, G.S. Dehydrogenation of $LiBH_4$ destabilized with various oxides. *J. Phys. Chem. C* **2009**, *113*, 17945–17949.
13. Chłopek, K.; Frommen, C.; Léon, A.; Zabara, O.; Fichtner, M. Synthesis and properties of magnesium tetrahydroborate, $Mg(BH_4)_2$. *J. Mater. Chem.* **2007**, *17*, 3496–3503.
14. Li, H.W.; Kikuchi, K.; Nakamori, Y.; Miwa, K.; Towata, S.; Orimo, S. Effects of ball milling and additives on dehydriding behaviors of well-crystallized $Mg(BH_4)_2$. *Scr. Mater.* **2007**, *57*, 679–682.
15. Newhouse, R.J.; Stavila, V.; Hwang, S.-J.; Klebanoff, L.E.; Zhang, J.Z. Reversibility and improved hydrogen release of magnesium borohydride. *J. Phys. Chem. C* **2010**, *114*, 5224–5232.

16. Mao, J.F.; Guo, Z.P.; Poh, C.K.; Ranjbar, A.; Guo, Y.H.; Yu, X.B.; Liu, H.K. Study on the dehydrogenation kinetics and thermodynamics of Ca(BH$_4$)$_2$. *J. Alloys Compd.* **2010**, *500*, 200–205.

17. Kim, Y.; Hwang, S.-J.; Lee, Y.S.; Suh, J.Y.; Han, H.N.; Cho, Y.W. Hydrogen back-pressure effects on the dehydrogenation reactions of Ca(BH$_4$)$_2$. *J. Phys. Chem. C* **2012**, *116*, 25715–25720.

18. Riktor, M.D.; Sørby, M.H.; Chopek, K.; Fichtner, M.; Haubac, B.C. The identification of a hitherto unknown intermediate phase CaB$_2$H$_x$ from decomposition of Ca(BH$_4$)$_2$. *J. Mater. Chem.* **2009**, *19*, 2754–2759.

19. Orimo, S.; Nakamori, Y.; Eliseo, J.; Züttel, A.; Jensen, C.M. Complex hydrides for hydrogen storage. *Chem. Rev.* **2007**, *107*, 4111–4132.

20. Li, H.W.; Yan, Y.G.; Orimo, S.; Züttel, A.; Jensen, C.M. Recent progress in metal borohydrides for hydrogen storage. *Energies* **2011**, *4*, 185–214.

21. Muir, S.S.; Yao, X.D. Progress in sodium borohydride as a hydrogen storage material: Development of hydrolysis catalysts and reaction systems. *Int. J. Hydrog. Energy* **2011**, *36*, 5983–5997.

22. U.S. Department of Energy Hydrogen Program. *Go/No-Go Recommendation for Sodium Borohydride for On-Board Vehicular Hydrogen Storage*; NREL/MP-150-42220; National Renewable Energy Laboratory (NREL): Golden, CO, USA, 2007.

23. Sigma-Aldrich. Available online: http://www.sigmaaldrich.com/united-states (accessed on 19 October 2014).

24. Santos, D.M.F.; Sequeira, C.A.C. Sodium borohydride as a fuel for the future. *Renew. Sustain. Energy Rev.* **2011**, *15*, 3980–4001.

25. Cakır, D.; Wijs, G.A.D.; Brocks, G. Native defects and the dehydrogenation of NaBH$_4$. *J. Phys. Chem. C* **2011**, *115*, 24429–24434.

26. Grochala, W.; Edwards, P. Thermal decomposition of the non-interstitial hydrides for the storage and production of hydrogen. *Chem. Rev.* **2004**, *104*, 1283–1315.

27. Mao, J.; Guo, Z.; Yu, X.; Liu, H. Improved hydrogen storage properties of NaBH$_4$ destabilized by CaH$_2$ and Ca(BH$_4$)$_2$. *J. Phys. Chem. C* **2011**, *115*, 9283–9290.

28. Garroni, S.; Milanese, C.; Pottmaier, D.; Mulas, G.; Nolis, P.; Girella, A.; Caputo, R.; Olid, D.; Teixdor, F.; Baricco, M.; *et al.* Experimental evidence of Na$_2$[B$_{12}$H$_{12}$] and Na formation in the desorption pathway of the 2NaBH$_4$ + MgH$_2$ System. *J. Phys. Chem. C* **2011**, *115*, 16664–16671.

29. Ngene, P.; van den Berg, R.; Verkuijlen, M.H.W.; de Jong, K.P.; de Jongh, P.E. Reversibility of the hydrogen desorption from NaBH$_4$ by confinement in nanoporous carbon. *Energy Environ. Sci.* **2011**, *4*, 4108–4115.

30. Friedrichs, O.; Remhof, A.; Hwang, S.-J.; Züttel, A. Role of Li$_2$B$_{12}$H$_{12}$ for the formation and decomposition of LiBH$_4$. *Chem. Mater.* **2009**, *22*, 3265–3268.

31. Caputo, R.; Garroni, S.; Olid, D.; Teixidor, F.; Suriñach, S.; Dolors Baró, M. Can Na$_2$[B$_{12}$H$_{12}$] be a decomposition product of NaBH$_4$? *Phys. Chem. Chem. Phys.* **2010**, *12*, 15093–15100.

32. Mao, J.F.; Guo, Z.P.; Nevirkovets, I.P.; Liu, H.K.; Dou, S.X. Hydrogen de-/absorption improvement of NaBH$_4$ catalyzed by titanium-based additives. *J. Phys. Chem. C* **2012**, *116*, 1596–1604.

33. Humphries, T.D.; Kalantzopoulos, G.N.; Llamas-Jansa, I.; Olsen, J.E.; Hauback, B.C. Reversible hydrogenation studies of NaBH$_4$ milled with Ni-containing additives. *J. Phys. Chem. C* **2013**, *117*, 6060–6065.

34. De Jongh, P.E.; Adelhelm, P. Nanosizing and nanoconfinement: New strategies towards meeting hydrogen storage goals. *ChemSusChem* **2010**, *3*, 1332–1348.

35. Varin, R.A.; Chiu, C. Structural stability of sodium borohydride (NaBH4) during controlled mechanical milling. *J. Alloys Compd.* **2005**, *397*, 276–281.

36. Ampoumogli, A.; Steriotis, T.; Trikalitis, P.; Giasafaki, D.; Bardaji, E.G.; Fichtner, M.; Charalambopoulou, G. Nanostructured composites of mesoporous carbons and boranates as hydrogen storage materials. *J. Alloys Compd.* **2011**, *509*, S705–S708.

37. Peru, F.; Garroni, S.; Campesi, R.; Milanese, C.; Marini, A.; Pellicer, E.; Baró, M.D.; Mulas, G. Ammonia-free infiltration of NaBH4 into highly-ordered mesoporous silica and carbon matrices for hydrogen storage. *J. Alloys Compd.* **2013**, *580*, S309–S312.

38. Christian, M.L.; Aguey-Zinsou, K.F. Core–shell strategy leading to high reversible hydrogen storage capacity for NaBH4. *ACS Nano* **2012**, *6*, 7739–7751.

39. Christian, M.L.; Aguey-Zinsou, K.F. Synthesis of core–shell NaBH4@M (M = Co, Cu, Fe, Ni, Sn) nanoparticles leading to various morphologies and hydrogen storage properties. *Chem. Commun.* **2013**, *49*, 6794–6796.

40. Zhang, L.T.; Xiao, X.Z.; Fan, X.L.; Li, S.Q.; Ge, H.W.; Wang, Q.D.; Chen, L.X. Fast hydrogen release under moderate conditions from NaBH4 destabilized by fluorographite. *RSC Adv.* **2014**, *4*, 2550–2556.

41. Mao, J.F.; Yu, X.B.; Guo, Z.P.; Liu, H.K.; Wu, Z.; Ni, J. Enhanced hydrogen storage performances of NaBH4–MgH2 system. *J. Alloys Compd.* **2009**, *479*, 619–623.

42. Garroni, S.; Pistidda, C.; Brunelli, M.; Vaughan, G.B.M.; Suriñach, S.; Baró, M.D. Hydrogen desorption mechanism of 2NaBH4 + MgH2 composite prepared by high-energy ball milling. *Scr. Mater.* **2009**, *60*, 1129–1132.

43. Dornheim, M. Tailoring Reaction Enthalpies of Hydrides. In *Handbook of Hydrogen Storage*; Hirscher, M., Ed.; Wiley-VCH: New York, NY, USA, 2010; pp. 187–214.

44. Mao, J.F.; Yu, X.B.; Guo, Z.P.; Poh, C.K.; Liu, H.K.; Wu, Z.; Ni, J. Improvement of the LiAlH4-NaBH4 system for reversible hydrogen storage. *J. Phys. Chem. C* **2009**, *113*, 10813–10818.

45. Afonso, G.; Bonakdarpour, A.; Wilkinson, D.P. Hydrogen storage properties of the destabilized 4NaBH4/5Mg2NiH4 composite system. *J. Phys. Chem. C* **2013**, *117*, 21105–21111.

46. Li, G.Q.; Matsuo, M.; Deledda, S.; Hauback, B.C.; Orimo, S. Dehydriding property of NaBH4 combined with Mg2FeH6. *Mater. Trans.* **2014**, *55*, 1141–1143.

47. Garroni, S.; Milanese, C.; Girell, A.; Marini, A.; Mulas, G.; Meneňdez, E.; Pistidda, C.; Dornheim, M.; Suriñach, S.; Baró, M.D. Sorption properties of NaBH4/MH2 (M = Mg, Ti) powder systems. *Int. J. Hydrog. Energy* **2010**, *35*, 5434–5441.

48. Pottmaier, D.; Pistidda, C.; Groppo, E.; Bordiga, S.; Spoto, G.; Dornheim, M.; Baricco, M. Dehydrogenation reactions of 2NaBH4 + MgH2 system. *Int. J. Hydrog. Energy* **2011**, *36*, 7891–7896.

49. Nwakwuo, C.C.; Pistidda, C.; Dornheim, M.; Hutchison, J.L.; Sykes, J.M. Microstructural analysis of hydrogen absorption in 2NaH + MgB2. *Scr. Mater.* **2011**, *64*, 351–354.

50. Pistidda, C.; Garroni, S.; Minella, C.; Dolci, F.; Jensen, T.R.; Nolis, P.; Bösenberg, U.; Cerenius, Y.; Lohstroh, W.; Fichtner, M.; *et al.* Pressure effect on the 2NaH + MgB2 hydrogen absorption reaction. *J. Phys. Chem. C* **2010**, *114*, 21816–21823.

51. Pistidda, C.; Pottmaier, D.; Karimi, F.; Garroni, S.; Rzeszutek, A.; Tolkiehn, M.; Fichtner, M.; Lohstroh, W.; Baricco, M.; Klassen, T.; *et al.* Effect of NaH/MgB$_2$ ratio on the hydrogen absorption kinetics of the system NaH + MgB2. *Int. J. Hydrog. Energy* **2014**, *39*, 5030–5036.

52. Garroni, S.; Minella, C.B.; Pottmaier, D.; Pistidda, C.; Milanese, C.; Marini, A.; Enzo, S.; Mulas, G.; Dornheim, M.; Baricco, M.; *et al.* Mechanochemical synthesis of NaBH$_4$ starting from NaH-MgB$_2$ reactive hydride composite system. *Int. J. Hydrog. Energy* **2013**, *38*, 2363–2369.

53. Pistidda, C.; Barkhordarian, G.; Rzeszutek, A.; Garroni, S.; Bonatto Minella, C.; Baró, M.D.; Nolis, P.; Bormann, R.; Klassen, T.; Dornheim, M. Activation of the reactive hydride composite 2NaBH$_4$ + MgH$_2$. *Scr. Mater.* **2011**, *64*, 1035–1038.

54. Mulas, G.; Campesi, R.; Garroni, S.; Napolitano, E.; Milanese, C.; Dolci, F.; Pellicer, E.; Baró, D.; Marini, A. Hydrogen storage in 2NaBH$_4$ + MgH$_2$ mixtures: Destabilization by additives and nanoconfinement. *J. Alloys Compd.* **2012**, *536*, S236–S240.

55. Lemke, C.H. Sodium and sodium alloys. In *Kirk-Othmer Encyclopedia of Chemical Technology*; John Wiley & Sons: New York, NY, USA, 1983; pp. 181–204.

56. Young, J.A. Sodium fluoride. *J. Chem. Educ.* **2002**, *79*, doi:10.1021/ed079p1197.

57. Yin, L.C.; Wang, P.; Kang, X.D.; Sun, C.H.; Cheng, H.M. Functional anion concept: Effect of fluorine anion on hydrogen storage of sodium alanate. *Phys. Chem. Chem. Phys.* **2007**, *9*, 1499–1502.

58. Rude, L.H.; Filsø, U.; D'Anna, V.; Spyratou, A.; Richter, B.; Hino, S.; Zavorotynska, O.; Baricco, M.; Sørby, M.H.; Hauback, B.C.; *et al.* Hydrogen–fluorine exchange in NaBH$_4$–NaBF$_4$. *Phys. Chem. Chem. Phys.* **2013**, *15*, 18185–18194.

59. Mao, J.F.; Guo, Z.P.; Liu, H.K.; Dou, S.X. Reversible storage of hydrogen in NaF–MB$_2$ (M = Mg, Al) composites. *J. Mater. Chem. A* **2013**, *1*, 2806–2811.

60. Zhang, Z.G.; Wang, H.; Zhu, M. Hydrogen release from sodium borohydrides at low temperature by the addition of zinc fluoride. *Int. J. Hydrog. Energy* **2011**, *36*, 8203–8208.

61. Kalantzopoulos, G.N.; Guzik, M.N.; Deledda, S.; Heyn, R.H.; Mullera, J.; Hauback, B.C. Destabilization effect of transition metal fluorides on sodium borohydride. *Phys. Chem. Chem. Phys.* **2014**, *16*, 20483–20491.

62. Chong, L.N.; Zou, J.X.; Zeng, X.Q.; Ding, W.J. Mechanisms of reversible hydrogen storage in NaBH$_4$ through NdF$_3$ addition. *J. Mater. Chem. A* **2013**, *1*, 3983–3991.

63. Zou, J.X.; Li, L.J.; Zeng, X.Q.; Ding, W.J. Reversible hydrogen storage in a 3NaBH$_4$/YF$_3$ composite. *Int. J. Hydrog. Energy* **2012**, *37*, 17118–17125.

64. Chong, L.N.; Zou, J.X.; Zeng, X.Q.; Ding, W.J. Effects of La fluoride and La hydride on the reversible hydrogen sorption behaviors of NaBH$_4$: A comparative study. *J. Mater. Chem. A* **2014**, *2*, 8557–8570.

65. Chong, L.N.; Zou, J.X.; Zeng, X.Q.; Ding, W.J. Study on reversible hydrogen sorption behaviors of a 3NaBH$_4$/HoF$_3$ composite. *Int. J. Hydrog. Energy* **2014**, *39*, 14275–14281.

66. Lu, J.; Fang, Z.Z.; Sohn, H.Y. A dehydrogenation mechanism of metal hydrides based on interactions between H$^{\delta+}$ and H$^-$. *Inorg. Chem.* **2006**, *45*, 8749–8754.

67. Chater, P.A.; Anderson, P.A.; Prendergast, J.W.; Walton, A.; Mann, V.S.J.; Book, D.; David, W.I.F.; Johnson, S.R.; Edwards, P.P. Synthesis and characterization of amide–borohydrides: New complex light hydrides for potential hydrogen storage. *J. Alloys Compd.* **2007**, *446–447*, 350–354.

68. Somer, M.; Acar, S.; Koz, C.; Kokal, I.; Hohn, P.; Cardoso-Gil, R.; Aydemir, U.; Akselrud, L. α- and β-Na2[BH4][NH2]: Two modifications of a complex hydride in the system NaNH2–NaBH4; syntheses, crystal structures, thermal analyses, mass and vibrational spectra. *J. Alloys Compd.* **2010**, *491*, 98–105.

69. Wu, C.; Bai, Y.; Yang, J.H.; Wu, F.; Long, F. Characterizations of composite NaNH2–NaBH4 hydrogen storage materials synthesized via ball milling. *Int. J. Hydrog. Energy* **2012**, *37*, 889–893.

70. Drozd, V.; Saxena, S.; Garimella, S.V.; Durygin, A. Hydrogen release from a mixture of NaBH4 and Mg(OH)2. *Int. J. Hydrog. Energy* **2007**, *32*, 3370–3375.

71. Varin, R.A.; Parviz, R. Hydrogen generation from the ball milled composites of sodium and lithium borohydride (NaBH4/LiBH4) and magnesium hydroxide (Mg(OH)2) without and with the nanometric nickel (Ni) additive. *Int. J. Hydrog. Energy* **2012**, *37*, 1584–1293.

72. Nakamori, Y.; Miwa, K.; Ninoyiya, A.; Li, H.; Ohba, N.; Towata, S.; Züttel, A.; Orimo, S. Correlation between thermodynamical stabilities of metal borohydrides and cation electronegativities: First-principles calculations and experiments. *Phys. Rev. B* **2006**, *74*, doi:10.1103/PhysRevB. 74.045126.

73. Nakamori, Y.; Li, H.W.; Kikuchi, K.; Aoki, M.; Miwa, K.; Towata, S.; Orimo, S. Thermodynamical stabilities of metal-borohydrides. *J. Alloys Compd.* **2007**, *446–447*, 296–300.

74. Seballos, L.; Zhang, J.Z.; Rönnebro, E.; Herbergd, J.L.; Majzoub, E.H. Metastability and crystal structure of the bialkali complex metal borohydride NaK(BH4)2. *J. Alloys Compd.* **2009**, *476*, 446–450.

75. Llamas-Jansa, I.; Aliouane, N.; Deledda, S.; Fonnelφp, J.E.; Frommen, C.; Humphries, T.; Lieutenant, K.; Sartori, S.; Sφrby, M.H.; Hauback, B.C. Chloride substitution induced by mechano-chemical reactions between NaBH4 and transition metal chlorides. *J. Alloys Compd.* **2012**, *530*, 186–192.

76. Černý, R.; Severa, G.; Ravnsbæk, D.B.; Filinchuk, Y.; D'Anna, V.; Hagemann, H.; Haase, D.; Jensen, C.M.; Jensen, T.R. NaSc(BH4)4: A novel scandium-based borohydride. *J. Phys. Chem. C* **2010**, *114*, 1357–1364.

77. Ravnsbæk, D.; Filinchuk, Y.; Cerenius, Y.; Jakobsen, H.J.; Besenbacher, F.; Skibsted, J.; Jensen, T.R. A series of mixed-metal borohydrides. *Angew. Chem. Int. Ed.* **2009**, *48*, 6659–6663.

78. Xia, G.L.; Li, L.; Guo, Z.P.; Gu, Q.F.; Guo, Y.H.; Yu, X.B.; Liu, H.K.; Liu, Z.W. Stabilization of NaZn(BH4)3 via nanoconfinement in SBA-15 towards enhanced hydrogen release. *J. Mater. Chem. A* **2013**, *1*, 250–257.

79. Ravnsbæk, D.B.; Ley, M.B.; Lee, Y.S.; Hagemann, H.; D'Anna, V.; Cho, Y.W.; Filinchuk, Y.; Jensen, T.R. A mixed-cation mixed-anion borohydride NaY(BH4)2Cl2. *Int. J. Hydrog. Energy* **2012**, *37*, 8428–8438.

80. Hummelshφj, J.S.; Landis, D.D.; Voss, J.; Jiang, T.; Tekin, A.; Bork, N.; Dułak, M.; Mortensen, J.J.; Adamska, L.; Andersin, J.; *et al.* Density functional theory based screening of ternary alkali-transition metal borohydrides: A computational material design project. *J. Chem. Phys.* **2009**, *131*, doi:10.1063/1.3148892.